

## Radiative emission study with the SOPHIA code in MISTRAL-B

A. Escarguel\*, F Rosmej, C. Brault, R. Stamm, Th. Pierre, D. Guyomarc'h, K. Quotb  
PIIM-UMR 6633 CNRS/Université de Provence, centre de St-Jérôme 13397 Marseille,  
France

\* email : alexandre.escarguel@up.univ-mrs.fr

### Abstract

Space resolved spectroscopic investigation of the helium driven MISTRAL-B plasma experiment have shown anomalous large emission of the singlet lines  $1s2s\ ^1S - 1snp\ ^1P$  compared to the triplet lines  $1s2p\ ^3P - 1snd\ ^3D$ . The theoretical analysis carried out with the SOPHIA code indicate that global effects of turbulence lead to a large perturbation of the singlet and triplet population of the neutral helium. First analysis of space resolved data are carried out.

The plasma created in the MISTRAL-B device is produced by a large multipolar plasma source operating an helium discharge in the main chamber (see figure 1) [1]. The discharge is sustained by hot tungsten filament emission. High energy electrons injected from the source produce the magnetized plasma column (solenoid S, with  $B_{\max} = 0.03\ \text{T}$ ; 1.2 m length, 40 cm diameter) with a large range of possible electron temperatures ( $0.5\ \text{eV} < T_e < 8\ \text{eV}$ ) and electron densities ( $n_e < 10^{12}\ \text{cm}^{-3}$ ). A limiter reduces the diameter of the plasma column to 3 cm. Two lines of sight, each one composed of a  $f=50\ \text{mm}$  lens and of an optical fiber (0.94 mm core diameter) allow to record the plasma light emission with a spectrometer device (1200 and 600  $\text{mm}^{-1}$  grooves, 50 cm focal length, 700 pixels intensified array detector, 32 Å or 16 Å/mm dispersion).  $T_e$  and  $n_e$  have been estimated from Langmuir probe measurements. Two configurations, giving different helium line spectra, are studied. In the first experiment, a transverse electric field created by two end collectors (FC and MC, in figure 1) with a relative biasing  $\Delta V$  leads to the  $E \times B$  extraction of a plasma jet in the shadow of the limiter L with ion velocities of a few km/s [2]. In the second configuration, only the positively polarized fixed collector FC is used at the end of the column. The left part of figure 2 shows the experimental spectra from MISTRAL in the spectral range from 320 nm until 380 nm: the singlet lines  $1s2s\ ^1S - 1snp\ ^1P_1$  for  $n=5-9$  and the triplet lines  $1s2p\ ^3P - 1snd\ ^3D$  for  $n=7-16$  are clearly visible. The upper and lower left spectra of Fig. 2 were observed in the first and second experimental configurations, respectively. The two spectra differ essentially in the relative intensity of the singlet line  $1s2s\ ^1S - 1s5p\ ^1P_1$  (indicated by arrow).

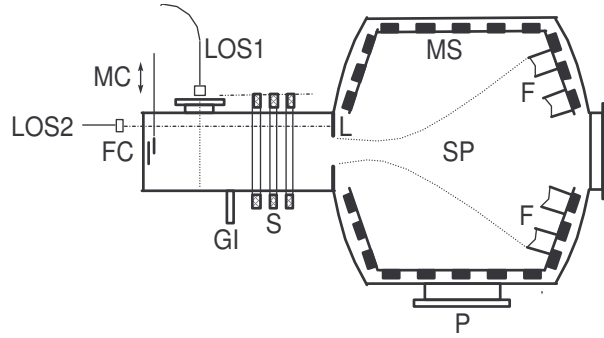


**Figure 1 : MISTRAL-B experimental device.** SP : source plasma ; gas injection ; F : filaments ; MS : ferrite magnets ; P : pumping system ; L : limiter ; S : solenoid ; GI : gas injection ; FC : fixed collector ; MC : moving collector ; LOS1 : line of sight 1 (radial observation) ; LOS2 : line of sight 2 (axial off axis observation).

Apart temperature and density diagnostics, the analysis of the radiation emission can deliver also information about various other plasma properties like charge state distribution, temporal and spatial variations, diffusion and flow processes, fluctuations, charge exchange, hot electrons [3, 4, 5]. Based on the relative intensity of the singlet and triplet lines, a diagnostic method has recently been developed to determine non-equilibrium conditions in the edge of magnetically confined fusion plasmas, JET [6] and in the NAGDIS-II divertor simulator experiment [7]. An important impact from the spectroscopic analysis stems from the fact, that it is based essentially on a collisional-radiative approach and therefore provides a plasma model independent information.

In order to simulate the radiative properties of the singlet and the triplet lines, the atomic levels included in the simulations have to be separated for both spin states up to very high quantum number. This is particularly complicated, as it also requests the whole atomic structure to be separated for the both spin directions. However, the available atomic database is too sparse for the most general approach : the collisional radiative model. The recently developed SOPHIA code [8] is devoted to these issues and involves an atomic level structure and atomic physics which separates the metastables and also the spin states up to very large principal quantum number ( $n = 30$ ). The spectral distribution  $I(\omega)$  of the line emission is calculated according:

$$I(\omega) = \sum_{i,j} I_{ij}(\omega) = \sum_{i,j} \hbar\omega_{ij} A_{ij} \Lambda_{ij} \Phi_{ij}(\omega). \quad (1)$$

$\Phi_{ij}$  is the normalized, optically-thick line-profile,  $\Lambda_{ij}$  the photon escape factor,  $A_{ji}$  the spontaneous radiative transition probability and  $\omega_{ij}$  is the transition frequency. The atomic-level population densities are determined from a system of rate equations:

$$\frac{dn_j}{dt} = \sum_{i=1}^N n_i \{ W_{ij} + A_{ij} \Lambda_{ij} \} - n_j \sum_{k=1}^N \{ W_{jk} + A_{jk} \Lambda_{jk} \}. \quad (2)$$

where  $n_j$  is the population density of state  $j$  ( $j$  runs over all levels including all ionisation stages). The elements of the collisional-radiative transition matrix  $W$  are given by

$$W_{ij} = C_{ij} + R_{ij} + I_{ij} + T_{ij} + \Gamma_{ij} + D_{ij}, \quad (3)$$

where  $C$  denotes the collisional excitation/deexcitation rate,  $I$  is the collisional ionisation rate,  $T$  is the 3-body recombination rate,  $R$  is the (spontaneous) radiative recombination rate,  $\Gamma$  is the auto-ionisation rate, and  $D$  is the radiationless electron capture rate. The matrix elements for the inverse processes are obtained by the application of the principle of detailed balance. If a particular transition cannot occur, because of energy or symmetry considerations, the corresponding rate is set equal to zero.

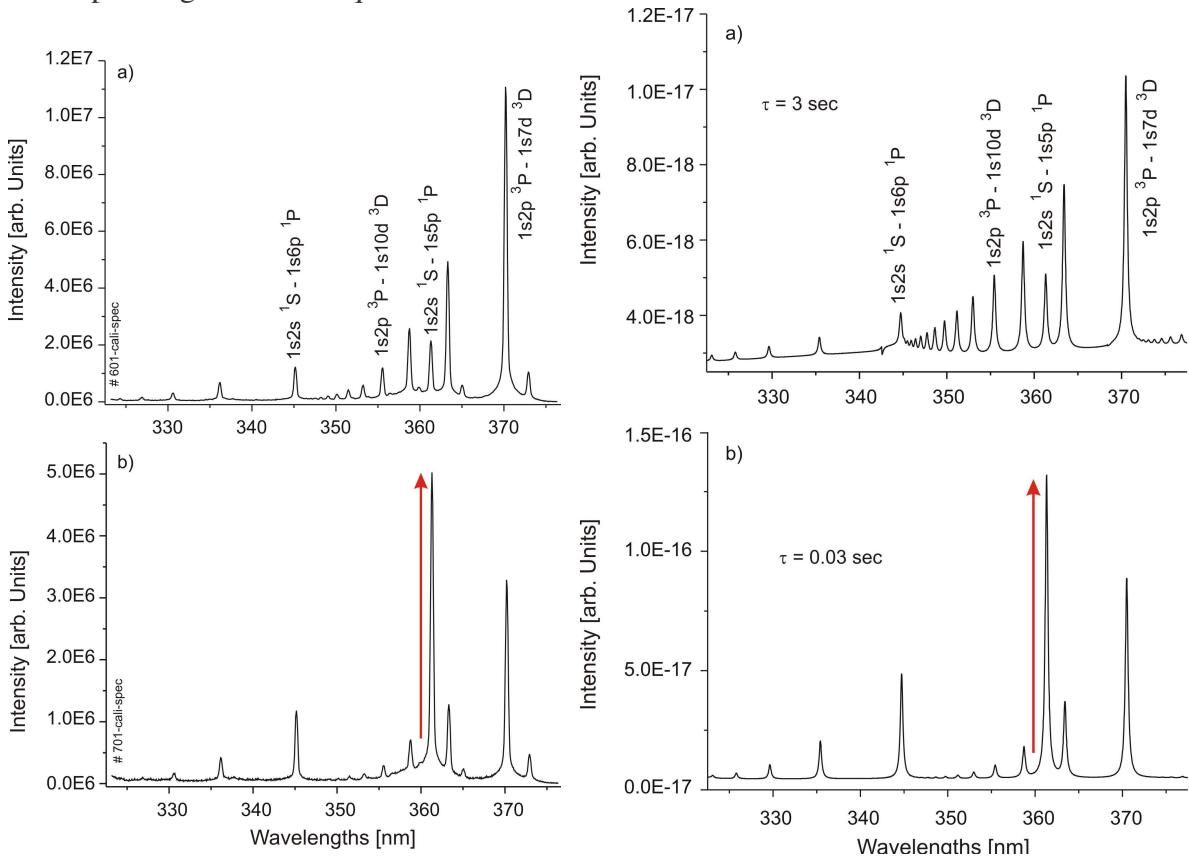


**Figure 2** : MISTRAL-B experimental spectra (**left**) and SOPHIA simulations (**right**) of neutral helium. **Upper left** : axial observation off axis ; **lower left** : radial observation. The two spectra differ largely (indicated by arrow) in the relative intensity of the singlet  $1s2s\ ^1S - 1s5p\ ^1P_1$  line and the triplet lines  $1s2p\ ^3P - 1s7d\ ^3D$ . **Upper and lower right** : SOPHIA simulations of the emission spectra of neutral helium for different  $\tau$  parameters.

Radiation transport effects are included self-consistently (causing eq. (2) to be non-linear) for all levels and ionisation stages. Non-equilibrium effects (see above) are calculated in  $\tau$ -approximation, i.e., the flux divergence term  $\nabla(n_j V)$  is replaced by  $\frac{n_j}{\tau}$ , i.e., loss terms for the ground states  $1s^2$ ,  $1s$  and nucleus are included in eq. (1). At present,  $\partial/\partial t = 0$  is assumed and the system eq. (1) is closed by normalization conditions (for more details see [3, 4]) :

$$\sum_{i,k} n_{i,k} = 1. \quad (4)$$

The indices run over all ionisation stages  $k$  ( $\text{He}^{++}$ ,  $\text{He}^+$ ,  $\text{He}^{0+}$ ) and all levels  $i$  present in the kinetic equation (1). One dimensional numerical calculations for a large set of diffusion coefficients and convective velocities indicate, that the  $\tau$ -approximation is able to keep track even of the details of the emission spectrum from metastable levels [3, 4].

The right part of figure 2 shows the spectral distribution obtained from the SOPHIA simulations for different  $\tau$  parameters : a)  $kT_e = 2.5$  eV,  $n_e = 3 \cdot 10^{10} \text{ cm}^{-3}$ ,  $L_{\text{eff}} = 3$  cm,  $\tau = 3$  sec, b)  $kT_e = 5$  eV,  $n_e = 3 \cdot 10^{10} \text{ cm}^{-3}$ ,  $\tau = 0.03$  sec. The simulations show a strong  $\tau$  dependence of the singlet and triplet lines. Comparison with the experimental spectra in Figure 2 shows, that the main features of the experimental spectra are displayed by the SOPHIA simulations. The essential difference between the two simulations of Fig. 2 is the about 2 orders of magnitude smaller  $\tau$  parameter for the radial observed spectra. A more quantitative analysis and interpolation of the  $\tau$  parameter in terms of diffusion, flow, charge exchange and hot electrons requests more precise knowledge of the temperature and density of the plasma column and its radial distribution which is envisaged for future experiments.

## References

- [1] C. Brault et al., 12<sup>th</sup> International Conference on Plasma Physics, Nice, France (2004)
- [2] A. Escarguel et al., 17<sup>th</sup> International Conference on Spectral Line Shape, Paris, (2004)
- [3] F.B. Rosmej and V.S. Lisitsa, Phys. Lett. A **244**, 401 (1998).
- [4] F.B. Rosmej et al, Plasma Physics and Controlled Fusion **41**, 191 (1999).
- [5] F. B. Rosmej, J. Phys. B Lett., **33**, L1 (2000)
- [6] F.B. Rosmej et al, 30<sup>th</sup> EPS Conference on Controlled Fusion and Plasma Physics, St. Petersburg, Russia, ECA, vol. 27A, P 1.176 (2003).
- [7] F.B. Rosmej et al., Journal of Nuclear Materials **337-339**, 1101 (2005).
- [8] F.B. Rosmej, to be published.